Evaluation of Temperature Effect on Benzene Density Using Molecular Dynamics Simulation

Abstract

In this study, molecular dynamics simulation has been conducted to model the density of pure benzene at 256.55-368.16 K temperature range and atmospheric pressure. All the simulations have been performed using BIOVIA Materials Studio 2017 software. The effects of various parameters on benzene density have been investigated, including the number of cell molecules (i.e., cell dimension), force field, and the initial cell density. Ewald and Atom-Based methods have been employed in the simulations to consider the electrostatic and van der Waals interactions. The molecular dynamics results were compared with the experimental data. Comparing the predicted and the experimental densities, the best results were obtained for 100 benzene molecules with COMPASS force field and the initial density of 0.9 times the experimental density. For initial densities of 70% and 90% of the experimental density, the coefficients of determination (R^2) were 0.9618 and 0.9779, and the RMSE values were 0.011269 and 0.0045548, respectively. The results indicate high accuracy of the molecular dynamics simulation for density prediction of pure benzene.

Keywords: Molecular Dynamics Simulation, Density, Benzene, COMPASS, Force Field, Materials Studio

1. Introduction

Molecular dynamics (MD) studies the interactions between atoms and molecules using equations of motion during a specific period [1-3]. It is a powerful tool for the description of molecular scaled properties [4] for different applications, such as mass transfer systems where the diffusivity and absorption may be described by MD models [5-9] or studying the structure, dynamics, and performance of biological molecules [10]. Molecular dynamics can provide the atomic details attributed to the dynamics of a simulated system under the conditions at which experimental measurements are difficult and expensive to obtain. Different methods based on molecular dynamics simulation could be implemented to compute the density of fluids for both

liquids and gasses [11]. Andersen developed the molecular dynamics simulation method while numerically solving the Hamiltonian equations of motion by averaging over isoenthalpic-isobaric canonical ensembles, taking the system volume into account as a dynamic variable [2]. Parinello and Rahman developed this method to let the cell shape change to investigate the effect of interaction potential on the crystal structure [1]. In addition, Nosé extended the MD method from isoenthalpic-isobaric canonical to canonical ensembles, and the constant temperature approach was created via time scaling in the system [3]. This approach gave rise to the equations of motion for the extended systems, which led to the extension of the Nosé thermostat and provided the isothermal-isobaric ensemble (NPT) equations [12].

Some techniques for optimizing the crystal structure parameters at high and low temperatures are vastly used [13]. Most MD programs in NPT ensembles have used planar wave bases. Also, for liquids, the equilibrium time of the NPT ensemble can be significantly longer because the volume fluctuations occur less frequently [14]. The mechanical force field (FF) is suitable for studying the condensed phase's characteristics [15-20]. Furthermore, the mechanical force field in atomic details can often go beyond the experiments. Even if a force field is attributed to studying the structures, dynamics, and functions of specific biomolecules, it is still crucial for the force field to precisely recreate the experimental liquid characteristics of small molecules that are the chemical constituents of the biomolecules. Wang et al. computed the density and heat of vaporization for an extensive system of organic molecules that contain distinct chemical functional groups [21]. They systematically predicted molecular characteristics (bulk density and vaporization heat) of 71 typical organic molecules via General AMBER Force Field (GAFF). In the MD simulation, they applied the Particle Mesh Ewald (PME) method to evaluate the electrostatic energy and used Langevin dynamics to control the temperature. The density average percent error (APE) compared to the experimental results was about 4.43%. By optimization of van der Waals parameters, they could dramatically enhance the predicted values of molecular properties.

In this study, the density of pure benzene was calculated by MD at the temperature range of 256.55-368.16 K and atmospheric pressure. The MD simulation results were compared with the experimental data of Brüsewitz et al. [22]. To predict the density of benzene, the effects of different parameters, including the number of cell molecules (cell dimension), force field, and initial density, have been studied. Then the difference between MD and experimental results

has been presented via the coefficient of determination (R^2) and the root mean squared error (RMSE).

2. Molecular dynamics simulation

All the simulations were carried out in this work using the Materials Studio 2017 software package. The amorphous cell module was used to apply periodic boundary conditions to determine the cell dimensions. In all the simulations, the COMPASS force field has been utilized to consider the molecular interactions in addition to Ewald and Atom-based summation methods for electrostatic and van der Waals interactions, respectively, with a cut-off distance of 12.5 Å. To construct the MD cell, first, the geometry of the benzene molecule has been optimized from the energy point of view to reach the most stable molecule. Afterward, the cell geometry was optimized. Fig. (1) shows the optimized benzene molecule and the optimized cell of 100 molecules.

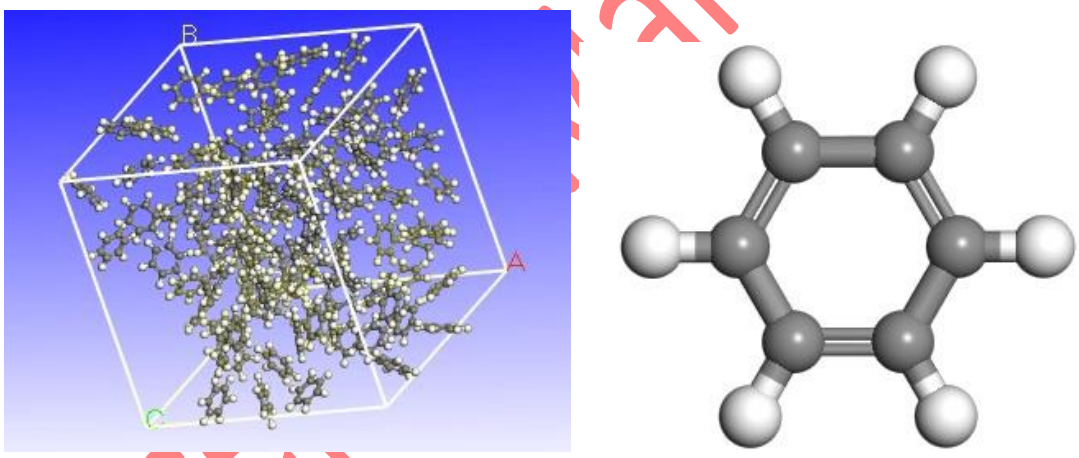

Fig. 1 The optimized molecule and cell of benzene.

The optimizations were conducted based on the minimization of the RMSE, and the predictions were assessed through the determination coefficient defined in Eqs. 1 and 2:

$$RMSE = \sqrt{\frac{\sum_{i=1}^{n}\left(\rho_i^{exp} - \rho_i^{sim}\right)^2}{n}} \quad (1)$$

$$R^2 = 1 - \frac{\sum_{i=1}^{n}\left(\rho_i^{exp} - \rho_i^{sim}\right)^2}{\sum_{i=1}^{n}\left(\rho_i^{sim} - \rho_m\right)^2} \quad (2)$$

where n is the number of data; $\rho_i^{\exp}$, ρ_m and ρ_i^{sim} present the experimental density, the average experimental density, and MD predicted density.

The benzene density was calculated using an NPT ensemble at the required temperature and pressure with a 1 fs time step. The velocity scale thermostat and Berendsen barostat were employed to control the temperature and pressure. The average density, ρ, was computed using the average volume of the simulation box, $\langle V \rangle$, using Eq. 3. In this equation, N_{res} is the number of remaining molecules in the cell, M is the studied molecule's molar mass, and N_A is the Avogadro constant.

$$\langle \rho \rangle = \frac{N_{res} M}{N_A \langle V \rangle} \tag{3}$$

2-1- Number of Molecules

To investigate the effect of the number of molecules or the cell dimension on density, first, the cell has been constructed with different molecule numbers at similar conditions (at the temperature of 298.15 K, the pressure of 1 atmosphere, and using COMPASS force field), and then the simulation results have been compared with the experimental data of Brüsewitz et al. [22]. The experimentally measured density of benzene at 298.15 K and 1 atmosphere is 0.8737 g/cm^3. As the number of molecules increases in the system, the value of simulated properties such as density approaches the bulk value. However, finding the optimum number of molecules that give rise to values close to the experimental results is crucial to reducing the simulation time and cost. Table 1 illustrates the number of molecules and the cell dimensions in different simulations. In addition, the initial cell density is 0.7 times the experimental density here. After the cell construction, the density was calculated using Eq. 3 at simulation times of 150, 200, 250, 300, 400, and 500 ps, and then the results were compared to the experimental data. Fig. (2-a) shows the MD predicted and the experimentally obtained densities versus the number of cell molecules at various simulation times.

Moreover, Fig. (2-b) shows the percentage of errors for predicted densities drawn versus the number of molecules at different times. As shown in Fig. (2-a), at all simulation times, the MD predicted density demonstrates a logarithmic increase as the number of molecules increases. The density variation is insignificant for the simulation cells with more than 80 benzene molecules. Fig. (2-b) reveals that the MD predicted density error compared to the experimental

one, is 10.3% for a cell with 80 molecules and at a simulation time of 300 ps. This error decreases to 6.73% for the cell with 100 molecules. Considering the slight difference between the predicted and the experimental values at 300 ps, for the 100-molecule cell, in the rest of the simulations, 100 molecules are used to construct the simulation box.

Table 1. The number of benzene molecules and the cell dimensions at 298.15K and the pressure of 1 atm.

No. of Molecules	Dimensions (Å)	No. of Molecules	Dimensions (Å)
3	8.6×8.6×8.6	80	25.7×25.7×25.7
5	10.2×10.2×10.2	100	27.7×27.7×27.7
10	12.8×12.8×12.8	150	31.7×31.7×31.7
20	16.2×16.2×16.2	200	34.9×34.9×34.9
40	20.4×20.4×20.4	300	39.9×39.9×39.9

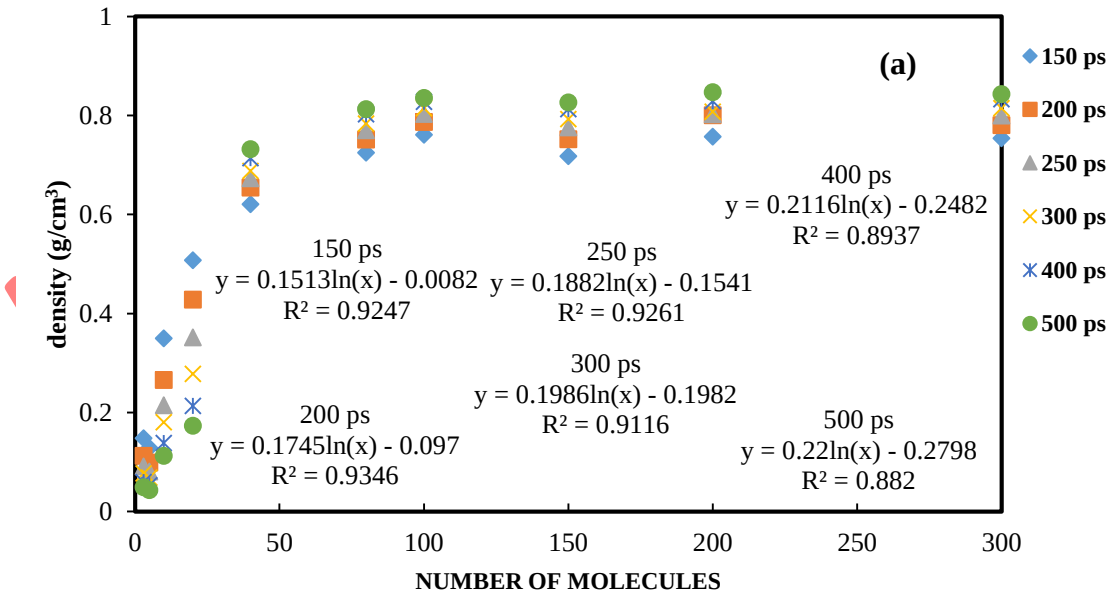

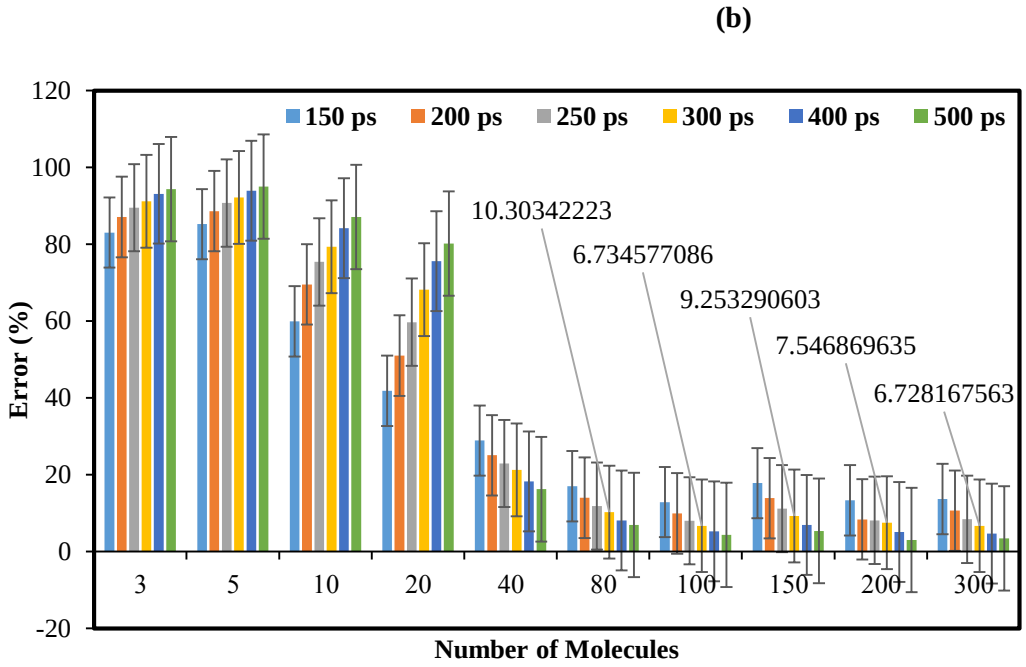

Fig. 2 a) Experimental and MD predicted densities vs. the number of cell molecules, b) the errors of the MD predicted densities vs. the number of cell molecules, at simulation times of 150, 200, 250, 300, 400, and 500 ps.

2-2- Optimized Force Field

After determining the optimum number of molecules for the prediction of the density of benzene at 298.15 K and 1 atm, the effect of the force field was investigated based on the previous work by Emamian et al. [19]. Benzene density was calculated for a constant number of molecules and at constant temperature and pressure using five different force fields, including COMPASS, Dreiding, Universal, Cvff, and Pcff, for simulation times between 150 and 300 ps. Fig. (3) represents the predicted and experimental densities at a simulation time of 300 ps at different applied force fields. Fig. (3) reveals that the absolute difference between the predicted and experimental density values is almost identical for both Universal and COMPASS force fields at t = 30 ps. However, as seen in Fig. (2-a), using COMPASS force field, in the worst case, the coefficient of determination (R^2) is 0.882 at 500 ps, while using Universal force

field, R^2 is 0.543. Therefore, 100 molecules and COMPASS force field were chosen for the rest of the simulations.

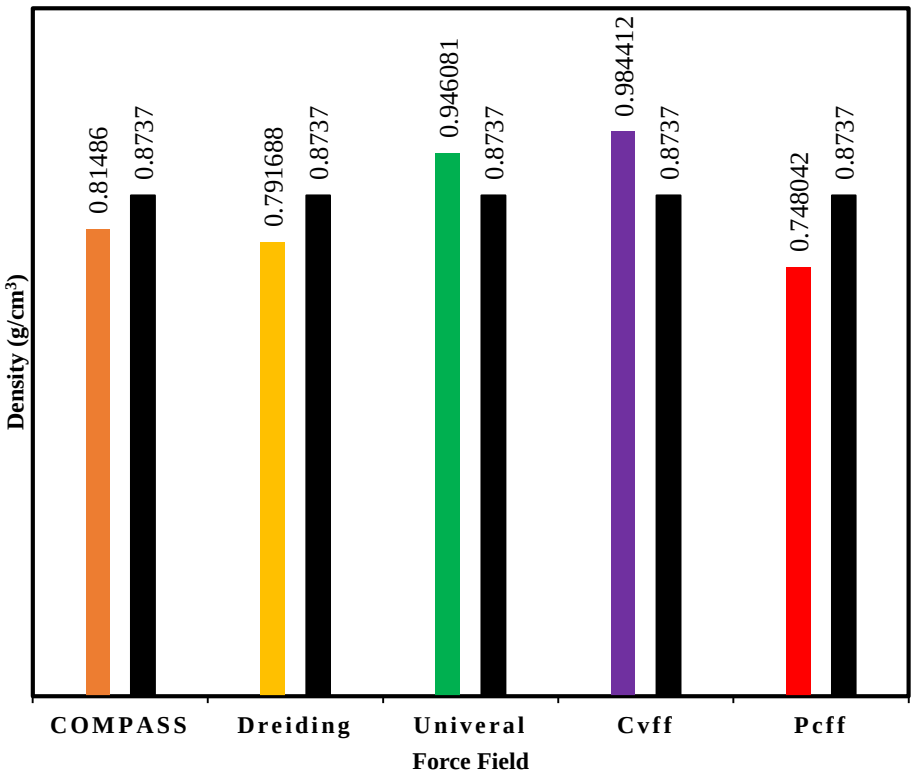

Fig. 3 Experimental (black column) and MD predicted densities at different force fields.

2-3- Initial Cell Density

During the cell construction, to predict the density using MD simulation, the initial cell density was 0.7 times the experimental density. Two initial densities of 0.7 ρ^{exp} and 0.9 ρ^{exp} (i.e., 0.61159 and 0.78633 g/cm^3) were used with simulation times of 150 – 500 ps to investigate the effect of the initial cell density on the ultimate predicted density. Fig. (4-a) shows the predicted and experimental densities versus simulation time at the initial densities. In contrast, Fig. (4-b) shows the percentage error versus simulation time for the initial densities mentioned. Fig. (4-a) shows that by increasing the initial cell density from 0.61159 to 0.78633 g/cm^3, the accuracy of the predicted density at similar simulation times has increased. Fig. (4-b) indicates that the percentage error decreases as the simulation time increases. Based on the results of Figs. (2-b) and (4-b), the simulation time of 300 ps was considered the optimum because it resulted in less

error. The error for the initial densities of 0.61159 and 0.78633 g/cm^3 are 6.37%, and 5.16%, respectively.

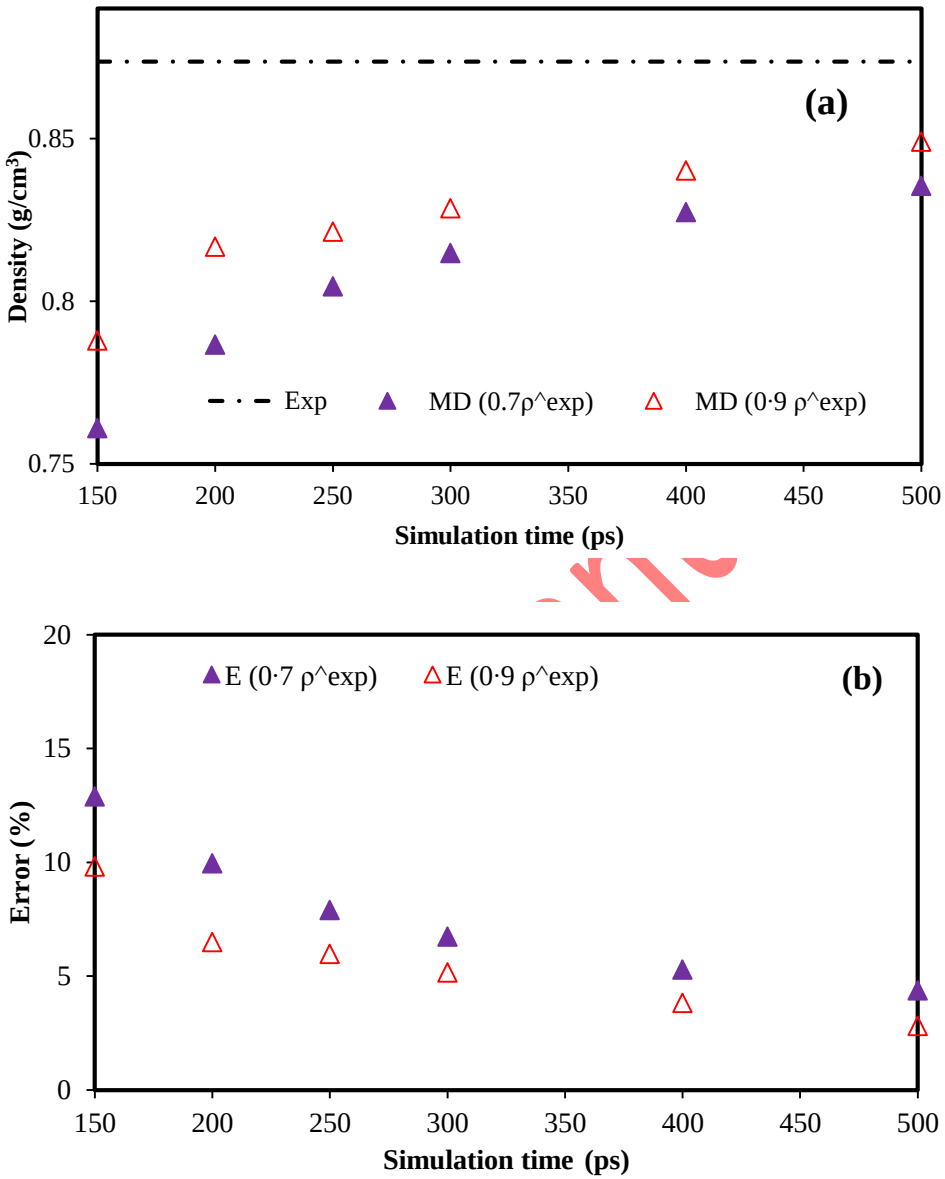

Fig. 4 The effect of a) initial cell density, b) percentage error vs. simulation time, at 298.15 K, 1 atm and COMPASS force field.

2-4- Temperature

For a molecular model, it is essential to accurately predict the molecular properties for a wide range of thermodynamic states. Each thermodynamic state is described by temperature, volume, and pressure [21]. In this part, benzene density was predicted for two initial densities of 0.7 ρ^{exp} and 0.9 ρ^{exp}, at the temperature range of 256.55 - 368.16 K. Then the results were

compared to the experimental results of Brüsewitz et al. [22]. Fig. (5) shows the MD predicted and experimental densities versus temperature. In general, as the temperature increases, the density decreases. As seen from Fig. (5), increasing the temperature gives rise to a decrease in experimental density and the predicted one for both initial densities. However, the results for 0.9 ρ^{exp} is closer to the experimental data as expected because as the system temperature increases, variation of electronic distribution in the system leads to the change of interaction between atoms, which is especially correct in metals but less accurate in semiconductors and insulators.

Consequently, in the current benzene cell, it is not expected to observe significant variation in the force field parameters, especially at the studied temperature range that is much less than the benzene band gap. Therefore, experimental and simulated densities similarly increase as the temperature rises. Table 2 illustrates R^2, RMSE, and APE for the two initial densities of 0.7 ρ^{exp} and 0.9 ρ^{exp}. The obtained APE and the results shown in Fig. (5-a) reveal that the predicted density using the initial density of 0.9 ρ^{exp} has given rise to more accurate results. Furthermore, R^2 values also indicate more accurate results for the initial density of 0.9 ρ^{exp} compared to 0.7 ρ^{exp}.

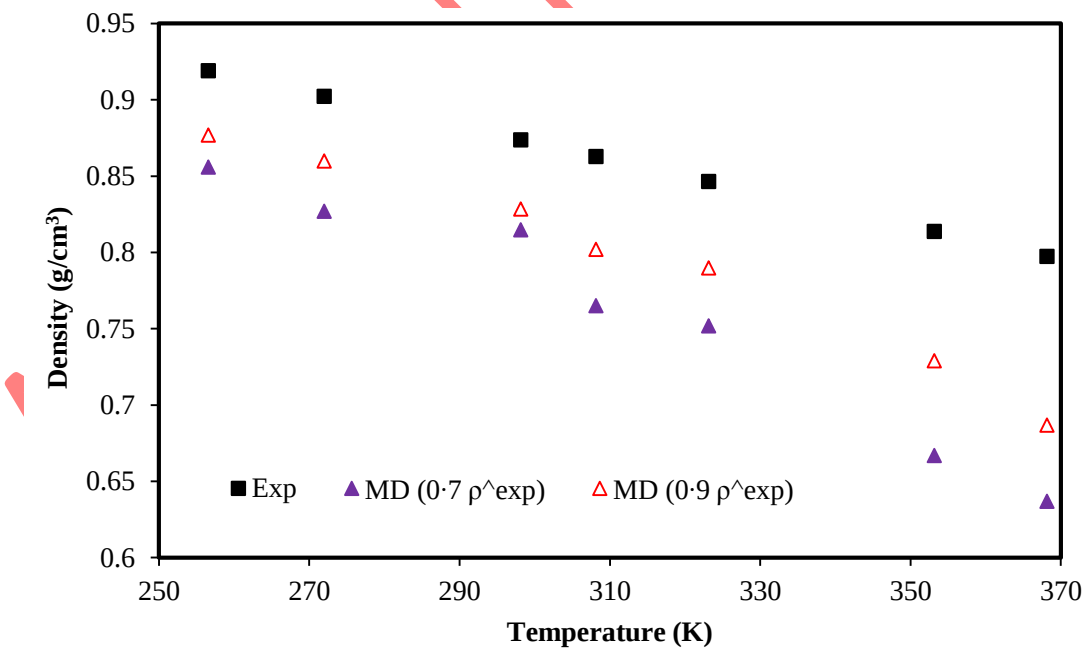

Fig. 5 The experimental and MD predicted benzene densities vs. temperature.

Table 2. R^2, RMSE and APE for two initial densities of 0.7 ρ^{exp} and 0.9 ρ^{exp}.

Initial densities	R^2	RMSE	APE
0.7 ρ^{exp}	0.9618	0.011269	11.79994
0.9 ρ^{exp}	0.9779	0.004555	7.49109

3. Conclusion

In this study, the effect of various parameters such as the number of cell molecules, force field, and initial density on the density prediction of pure benzene was studied at the temperature of 298.15 K and the pressure of 1 atmosphere. The predicted results have been compared to the experimental data. After finding the optimized conditions of 100 benzene molecules and COMPASS force field, the density of benzene has been calculated at the temperature range of 256.55 – 368.16 K and atmospheric pressure for two initial densities of 0.7 and 0.9 times the experimental density. The difference between the MD predicted, and the experimental results were described using the coefficient of determination, root mean squared error, and average percentage error. At optimized conditions, for two initial densities of 0.7 ρ^{exp} and 0.9 ρ^{exp}, R^2 values have been computed as 0.9618 and 0.9779, and the correspondent RMSEs were obtained as 0.01127 and 0.0046, respectively.

References

1. Parrinello, M. and A. Rahman, *Crystal Structure and Pair Potentials: A Molecular-Dynamics Study.* Physical Review Letters, 1980. **45**(14): p. 1196-1199.
2. Andersen, H.C., *Molecular dynamics simulations at constant pressure and/or temperature.* The Journal of Chemical Physics, 2008. **72**(4): p. 2384-2393.
3. Nosé, S., *A unified formulation of the constant temperature molecular dynamics methods.* The Journal of Chemical Physics, 1984. **81**(1): p. 511-519.
4. van Gunsteren, W.F. and A.E. Mark, *Validation of molecular dynamics simulation.* The Journal of Chemical Physics, 1998. **108**(15): p. 6109-6116.
5. Moradi, H., et al., *Effect of Si/Al ratio in Faujasite structure on adsorption of methane and nitrogen: A molecular dynamics study.* Chemical Engineering & Technology, 2021. **44**.
6. Moradi, H., et al., *Molecular dynamics simulation of H2S adsorption behavior on the surface of activated carbon.* Inorganic Chemistry Communications, 2020. **118**: p. 108048.
7. Emamian, M., et al., *Performance of molecular dynamics simulation for predicting of solvation free energy of neutral solutes in methanol.* Chemical Product and Process Modeling, 2021. **17**.
8. Moradi, H., et al., *Prediction of methane diffusion coefficient in water using molecular dynamics simulation.* Heliyon, 2020. **6**(11): p. e05385.
9. Tavan, Y., L. Jafari, and H. Moradi, *A theoretical and industrial study of component co-adsorption on 3A zeolite: An industrial case.* Chemical Papers, 2019.
10. Karplus, M. and J.A. McCammon, *Molecular dynamics simulations of biomolecules.* Nat Struct Biol, 2002. **9**(9): p. 646-52.

11. Alejandre, J., D.J. Tildesley, and G.A. Chapela, *Molecular dynamics simulation of the orthobaric densities and surface tension of water.* The Journal of Chemical Physics, 1995. **102**(11): p. 4574-4583.
12. Nosé, S. and M.L. Klein, *Constant pressure molecular dynamics for molecular systems.* Molecular Physics, 1983. **50**(5): p. 1055-1076.
13. Gillan, M.J., et al., *First-principles modelling of Earth and planetary materials at high pressures and temperatures.* Reports on Progress in Physics, 2006. **69**: p. 2365-2441.
14. Schmidt, J., et al., *Isobaric−Isothermal Molecular Dynamics Simulations Utilizing Density Functional Theory: An Assessment of the Structure and Density of Water at Near-Ambient Conditions.* The Journal of Physical Chemistry B, 2009. **113**(35): p. 11959-11964.
15. Cerezo, J., et al., *Adiabatic-Molecular Dynamics Generalized Vertical Hessian Approach: A Mixed Quantum Classical Method To Compute Electronic Spectra of Flexible Molecules in the Condensed Phase.* J Chem Theory Comput, 2020. **16**(2): p. 1215-1231.
16. Grimme, S., et al., *A general intermolecular force field based on tight-binding quantum chemical calculations.* J Chem Phys, 2017. **147**(16): p. 161708.
17. Grimme, S., *A General Quantum Mechanically Derived Force Field (QMDFF) for Molecules and Condensed Phase Simulations.* Journal of Chemical Theory and Computation, 2014. **10**(10): p. 4497-4514.
18. Zhang, C., et al., *Polarizable Multipole-Based Force Field for Aromatic Molecules and Nucleobases.* Journal of Chemical Theory and Computation, 2017. **13**(2): p. 666-678.
19. Giese, T.J. and D.M. York, *Quantum mechanical force fields for condensed phase molecular simulations.* Journal of Physics: Condensed Matter, 2017. **29**(38): p. 383002.
20. Harrison, J., et al., *Review of force fields and intermolecular potentials used in atomistic computational materials research.* Applied Physics Reviews, 2018. **5**: p. 031104.
21. Wang, J. and T. Hou, *Application of Molecular Dynamics Simulations in Molecular Property Prediction. 1. Density and Heat of Vaporization.* Journal of Chemical Theory and Computation, 2011. **7**(7): p. 2151-2165.
22. Michael, B. and W. Alarich, *Pressure-Temperature-Dependence of Mass Density and Self-Diffusion Coefficients in the Binary Liquid System n-Hexane/Benzene.* Berichte der Bunsengesellschaft für physikalische Chemie, 1990. **94**(3): p. 386-391.